

Electron transfer theory revisit: Quantum solvation effect

Ping Han,^{a,c)} Rui-Xue Xu,^{b,c)*} Ping Cui,^{c)} Yan Mo,^{c)} Guozhong He,^{a)} and YiJing Yan^{a,b,c)*}

^{a)}State Key Laboratory of Molecular Reaction Dynamics,

Dalian Institute of Chemical Physics, Chinese Academy of Sciences, Dalian 116023, China

^{b)}Hefei National Laboratory for Physical Sciences at the Microscale,

University of Science and Technology of China, Hefei 230026, China

^{c)}Department of Chemistry, Hong Kong University of Science and Technology, Kowloon, Hong Kong

(Dated: Accepted 25 May 2006, *J. Theo. & Comput. Chem.*; manu#: jtcc06052a)

The effect of solvation on ET rate processes is investigated on the basis of the exact theory constructed in *J. Phys. Chem. B* **110**, xxx (2006). The nature of solvation is studied in a close relation with the mechanism of ET processes. The resulting Kramers' turnover and Marcus' inversion characteristics are analyzed accordingly. The classical picture of solvation is found to be invalid when the solvent longitudinal relaxation time is short compared with the inverse temperature.

I. INTRODUCTION

Chemical reaction in condensed phases is intimately related to the Brownian motion in solution. Einstein's paper on Brownian motion¹ showed the first time the fluctuation-dissipation relation (FDR). The fluctuations of surrounding molecules are responsible for both agitation and friction on the Brownian particle. These stochastic events of energy exchange between system and bath lead eventually to thermal equilibrium. Brownian motion is characterized by the stochastic force. The FDR leads to a Fokker-Planck equation, which is the classical reduced equation of motion that governs the Brownian motion at an ensemble average level. This approach has been exploited by Kramers in his construction of isomerization reaction rate theory.² The resulting rate is shown to have a maximum in an intermediate viscosity region. This celebrated Kramers' turnover behavior clearly demonstrates the dual role of solvent on reaction rate.^{2,3}

Electron transfer (ET) is the simplest but a pivotally important chemical reaction system. It constitutes another class of systems whose dependence on solvent environment has been extensively studied since the pioneering work by Marcus in 1950s.^{4,5,6,7,8,9,10,11,12,13,14,15,16,17,18,19,20} However, it is often treated in different way from the traditional chemical reaction involving bond breaking and/or formation. In the latter case, either the equation of motion for a particle over the barrier or the flux-flux correlation function approach on the basis of the transition-state theory is used.^{3,21,22,23} The standard treatment in the ET research field is rather a type of transfer coupling correlation function formalism, based on the assumption that the nonadiabatic coupling matrix element V is not strong.^{4,5,6,7,8,9,10,11,12,13,14,15,16,17,18,19,20}

Depicted in Fig. 1 is the schematics of an elementary donor-acceptor ET system. Here, E° denotes the reaction endothermicity; V_a (V_b) represents the potential surface of the solvent environment for the electron in the donor (acceptor) state; $U \equiv V_b - V_a - E^\circ$ is the solvation coordinate; while $\lambda \equiv \langle U \rangle$ is the solvation energy, with $\langle \dots \rangle$ denoting the initial bath ensemble average. At the

crossing ($U + E^\circ = 0$) point, $V_a = V_b = (E^\circ + \lambda)^2/(4\lambda)$ that amounts to the ET reaction barrier height. The celebrated Marcus' rate theory reads^{4,5,6}

$$k = \frac{V^2/\hbar}{\sqrt{\lambda k_B T/\pi}} \exp \left[-\frac{(E^\circ + \lambda)^2}{4\lambda k_B T} \right]. \quad (1)$$

It is a classical Franck-Condon theory, assuming that the solvent relaxation is much slow compared with the electronic transition. Exploited in Eq. (1) is also the classical FDR: $\langle U^2 \rangle - \langle U \rangle^2 = 2k_B T \langle U \rangle$. Quantum extension of Marcus' theory has been formulated in the weak transfer coupling regime.^{19,20} The dynamic solvation effect is introduced by the solvation correlation function,

$$C(t) = \langle U(t)U(0) \rangle - \langle U \rangle^2. \quad (2)$$

Nonperturbative rates have also been formulated on the basis of fourth-order transfer correlation functions, followed by certain resummation schemes to partially account for the nonperturbative transfer coupling effects.^{9,10,11,12,13,14,15,16,17,18} The resulting rates, despite of the resummation approximation involved, do recover the celebrated Kramers' turnover behavior.

The main purpose of this work is to elucidate some distinct solvation effects on the ET rate processes. The quantum nature of solvation arises from the fact that the solvation coordinate is an operator and its correlation function must be complex. The elementary ET system in Debye solvents will be studied on the basis of the exact and analytical rate theory developed in Ref. 24, which will be referred as Paper I hereafter. Section II summarizes the theoretical results of Paper I. This is a reduced quantum equation of motion based formalism; i.e., the quantum version of Kramers' Fokker-Planck equation approach. The key quantity now is the reduced density matrix, $\rho(t) = \text{tr}_B \rho_{\Gamma}$, defined as the trace of the total system-bath density matrix over the bath subspace. Numerical results will be presented and discussed in Sec. III. Finally, Sec. IV concludes this paper.

II. AN EXACT AND ANALYTICAL THEORY

This section summarizes the exact and analytical rate theory, developed in Paper I, for the ET in Debye solvents at finite temperatures. Let us start with the following form of the reduced Liouville equation,

$$\dot{\rho}(t) = -\frac{i}{\hbar}[H, \rho(t)] - \int_0^t d\tau \hat{\Pi}(t, \tau) \rho(\tau). \quad (3)$$

For the present ET system (Fig. 1), the reduced system Hamiltonian reads

$$H = (E^\circ + \lambda)|b\rangle\langle b| + V(|a\rangle\langle b| + |b\rangle\langle a|). \quad (4)$$

This is a time-independent system, for which the dissipation memory kernel $\hat{\Pi}(t, \tau) = \hat{\Pi}(t - \tau)$. As a result, Eq. (3) can be resolved in its Laplace domain as

$$s\tilde{\rho}(s) - \rho(0) = -i\mathbf{L}\tilde{\rho}(s) - \Pi(s)\tilde{\rho}(s). \quad (5)$$

Here $\mathbf{L} \equiv \hbar^{-1}[H, \bullet]$ is the reduced system Liouvillian.

A simplification arises for the ET system in Debye solvents at finite temperature. The solvation correlation function assumes now (for $t > 0$)

$$C(t) = \lambda(2k_B T - i\hbar\gamma)e^{-\gamma t} \equiv \hbar^2\eta e^{-t/\tau_L}. \quad (6)$$

Here, $\tau_L \equiv \gamma^{-1}$ denotes the longitudinal relaxation time of the Debye solvent. In this case, Eq. (5) can be formulated exactly in terms of a continued fraction Green's function formalism. Let $\Pi(s) \equiv \Pi^{(0)}(s)$ and

$$\mathcal{G}^{(n)}(s) \equiv \frac{1}{s + i\mathbf{L} + \Pi^{(n)}(s)}; \quad n \geq 0. \quad (7)$$

The continued fraction hierarchy is now the relation between $\Pi^{(n)}(s)$ and $\mathcal{G}^{(n+1)}(s + \gamma)$; cf. the eq (16) of Paper I. For the elementary ET system subject to the Debye longitudinal relaxation, it is found that $\Pi^{(n)}$, which is Hermite satisfying $\Pi_{jj',kk'}^{(n)} = \Pi_{j'j,k'k}^{(n)*}$, has only three nonzero tensor elements together with their complex conjugates. Denote the three nonzero tensor elements of $\Pi^{(n)}$ as

$$x \equiv \Pi_{ba,ba}, \quad y \equiv \Pi_{ba,ab}, \quad z \equiv \Pi_{ba,bb}. \quad (8)$$

Implied here, and also whenever applicable hereafter [cf. Eqs. (10a)–(11b)], are the superscript index (n) and argument s , if they are the same in the both sides of the individual equation; otherwise they will be specified. The continued fraction hierarchy that relates $\Pi^{(n)}(s)$ with $\mathcal{G}^{(n+1)}(s + \gamma)$ can now be expressed in terms of

$$x^{(n)}(s) = \eta(n+1)X^{(n+1)}(s + \gamma), \quad (9a)$$

$$y^{(n)}(s) = -\eta^*(n+1)Y^{(n+1)}(s + \gamma), \quad (9b)$$

$$z^{(n)}(s) = (\eta - \eta^*)(n+1)Z^{(n+1)}(s + \gamma). \quad (9c)$$

Here, $\{X, Y, Z\}^{(n)}(s)$ are the counterpart tensor elements of the Green's function $\mathcal{G}^{(n)}(s)$. Their relations to the

nonzero elements $\{x, y, z\}^{(n)}(s)$ of $\Pi^{(n)}(s)$ via Eq. (7) can be evaluated analytically on the basis of the Dyson equation technique. The final results are

$$X \equiv \mathcal{G}_{ba,ba} = \frac{\alpha^* + \beta^*}{|\alpha + \beta|^2 - |\beta - y|^2}, \quad (10a)$$

$$Y \equiv \mathcal{G}_{ba,ab} = \frac{\beta - y}{|\alpha + \beta|^2 - |\beta - y|^2}, \quad (10b)$$

$$Z \equiv \mathcal{G}_{ba,bb} = -\frac{1}{s}[(z - iV/\hbar)X + (z^* + iV/\hbar)Y], \quad (10c)$$

with

$$\alpha \equiv s + (i/\hbar)(E^\circ + \lambda) + x, \quad (11a)$$

$$\beta \equiv s^{-1}(V/\hbar)^2[2 + i\hbar z/V]. \quad (11b)$$

The kinetics rate equation can be readily obtained via Eq. (5) by eliminating the off-diagonal reduced density matrix elements. It leads to a linear algebraic equation in the Laplace domain that corresponds to the generalized rate equation with memory rate kernels in time domain. The resulting ET rate resolution reads as [the eq (36a) of Paper I]

$$k(s) = \frac{2|V|^2}{\hbar^2} \text{Re} \frac{\alpha(s) + y(s)}{|\alpha(s)|^2 - |y(s)|^2}. \quad (12)$$

The rate constant $k \equiv k(0)$ that will be numerically studied in the next section amounts to the time integral of the memory rate kernel in the aforementioned generalized rate equation.

As analyzed in Paper I, the infinity inverse recursive formalism [Eqs. (9) and (10)] can be truncated by setting $\{x, y, z\}^{(N)} = 0$ at a sufficiently large anchoring N . The resulting $\{x, y, z\}^{(0)} \equiv \{x, y, z\}$ that are required by Eq. (12) are exact up to the $(2N)^{\text{th}}$ -order in the system-bath coupling. The convergence is guaranteed also via the mathematical continued fraction structure involved. Apparently, if the rates are needed at a specified s' , one shall start with $\{x, y, z\}_{s=s'+N\gamma}^{(N)} = 0$. The backward-recursion relations, Eqs. (9) with Eqs. (10), will then lead to $\{x, y, z\}_{s=s'+(N-1)\gamma}^{(N-1)}$, and so on, until $\{x, y, z\}_{s=s'}^{(0)} \equiv \{x, y, z\}_{s=s'}$ are reached for evaluating the required $k(s')$ [Eq. (12)]. The above reduced dynamics-based ET rate formalism is exact for the Debye solvents in finite temperatures. However, the FDR, which relates the real and imaginary parts of the solvation correlation function, is adopted in Eq. (6) in a semiclassical manner. As a consequence the reduced density matrix and rates may become negative if the temperature is too low.

III. QUANTUM SOLVATION EFFECTS: NUMERICAL RESULTS

We are now in the position to elucidate some distinct solvation effects on the ET reaction rate $k \equiv k(s=0)$ [cf. Eq. (12)]. Numerical results will be presented in relation

to the celebrated Kramers' turnover and Marcus' inversion behaviors, exemplified with the ET reaction systems of $V = 1$ kJ/mol and $\lambda = 3$ kJ/mol at $T = 298$ K.

It is noticed that the solvation longitudinal relaxation time τ_L is considered proportional to the solvent viscosity.^{16,17} The Kramers' turnover characteristics can therefore be demonstrated in terms of the rate k as a function of the scaled solvent relaxation time $\tau_L/\tau_{\text{ther}}$. Here, $\tau_{\text{ther}} \equiv \hbar/(k_B T)$ denotes the thermal time, which at the room temperature is about 26 fs. In the Debye solvent model of Eq. (6), the quantum nature of solvation enters via the semiclassical FDR that relates the real and imaginary parts of the correlation function. In contrast, the classical solvation is characterized by the real part only. As $\text{Im}\eta/\text{Re}\eta = -0.5\tau_{\text{ther}}/\tau_L$, it is anticipated that the quantum nature of solvation can only be prominent in the low viscosity ($\tau_L < \tau_{\text{ther}}$) regime. It is also consistent with the physical picture that the high viscosity (or slow motion) implies a large effective mass and thus leads to the classical solvation limit.

Figure 2 depicts the rates k as functions of $\tau_L/\tau_{\text{ther}}$ for two typical systems, being of the endothermicity values of $E^\circ = -\lambda$ and $E^\circ = 0$, respectively. Observed in the high viscosity ($\tau_L/\tau_{\text{ther}} > 1$) regime for each of the systems is the celebrated Kramers' fall-off behavior.^{2,3} This is the well established classical solvation picture of the diffusion limit: the higher the solvent viscosity is, the more backscattering (or barrier-recrossing) events will be. The fact that $k_{E^\circ=-\lambda} > k_{E^\circ=0}$ observed in the high viscosity regime is also anticipated from the classical solvation picture [cf. Fig. 1 or Eq. (1)]: That $E^\circ = -\lambda$ represents a classical barrierless system where the celebrated Marcus' inversion takes place.

In the low viscosity ($\tau_L/\tau_{\text{ther}} < 1$) regime the classical picture of solvation is however invalid. The observed rate in the symmetric ($E^\circ = 0$) system, is apparently tunneling dominated due to Fermi resonance. The most striking observation is that the so called barrierless ($E^\circ = -\lambda$) system exhibits now clearly the Kramers' viscosity-assisted barrier-crossing characteristics in the low viscosity regime. This suggests that there is an effective barrier for the ET system with the classical barrierless value of $E^\circ + \lambda = 0$; this effective barrier is viscosity dependent and vanishes as τ_L increases.

Now turn to the Marcus' inversion characteristics for the rate k as a function of reaction endothermicity E° . Depicted in Fig. 3 are the resulting inversion curves, with $\tau_L/\tau_{\text{ther}} = 0.1, 1$, and 10 to represent the low (solid-curve), intermediate (dot-curve), and high (dash-curve) viscosity regimes, respectively. In the classical solvation picture the inversion occurs at $E^\circ = -\lambda$, as it represents

a classical barrierless system. This picture is only valid in the high viscosity regime; see the dashed curve with $\tau_L/\tau_{\text{ther}} = 10$.

In the low viscosity regime, according to the analysis presented for Fig. 2, there is always a nonzero barrier for the ET reaction, covering over the entire range of E° including the value of $E^\circ = -\lambda$. This explains the inversion behavior of the solid curve in Fig. 3 that is peaked only at the resonant position of $E^\circ = 0$. As the viscosity increases, the inversion region smoothly shifts from the resonant peak position $E^\circ = 0$ to the classical barrierless position of $E^\circ = -\lambda$.

To explain the asymmetric property of the inversion behavior observed in Fig. 3, let us recall that $k(-E^\circ)$ amounts to the backward reaction rate and $k(E^\circ) < k(-E^\circ)$ for an endothermic ($E^\circ > 0$) reaction. This leads immediately to the asymmetric property of the solid curve in Fig. 3, in which the blue (endothermic) wing falls off faster than its red (exothermic) wing. The degree of asymmetry decreases as the viscosity increases. Only in the high viscosity regime does the inversion curve behave classically, which is symmetric (but may not be parabolic unless the transfer coupling V is small) around its classical inversion position of $E^\circ = -\lambda$.

IV. SUMMARY

In summary, we have investigated in detail the effect of solvation on ET rate processes. The nature of solvation is studied in a close relation with the mechanism of ET processes in terms of Kramers' turnover and Marcus' inversion characteristics. The classical picture of solvation is found to be invalid in the low viscosity regime, which can be well measured by the scaled longitudinal relaxation time of $\tau_L/\tau_{\text{ther}}$, where $\tau_{\text{ther}} = \hbar/(k_B T)$ is the thermal time. The present study is carried out on the basis of the exact rate theory for the simplest ET system with a single solvation relaxation time scale. Nevertheless, the basic results obtained here are expected to be valid to a general ET system in a realistic solvent environment of multiple relaxation time scales.

Acknowledgments

Support from the RGC Hong Kong and the NNSF of China (No. 50121202, No. 20403016 and No. 20533060) and Ministry of Education of China (no. NCET-05-0546) is acknowledged.

* Electronic address: rxxu@ustc.edu.cn; yyan@ust.hk

¹ A. Einstein, *Ann. Phys.* **7**, 549 (1905).

² H. A. Kramers, *Physica (Amsterdam)* **7**, 284 (1940).

³ P. Hänggi, P. Talkner, and M. Borkovec, *Rev. Mod. Phys.*

62, 251 (1990).

⁴ R. A. Marcus, *J. Chem. Phys.* **24**, 966 (1956).

⁵ R. A. Marcus, *Annu. Rev. Phys. Chem.* **15**, 155 (1964).

⁶ R. A. Marcus and N. Sutin, *Biochim. Biophys. Acta* **811**,

- 265 (1985).
- ⁷ L. D. Zusman, Chem. Phys. **49**, 295 (1980).
 - ⁸ L. D. Zusman, Chem. Phys. **80**, 29 (1983).
 - ⁹ J. T. Hynes, Annu. Rev. Phys. Chem. **36**, 573 (1985).
 - ¹⁰ A. Garg, J. N. Onuchic, and V. Ambegaokar, J. Chem. Phys. **83**, 4491 (1985).
 - ¹¹ H. Frauenfelder and P. G. Wolynes, Science **229**, 337 (1985).
 - ¹² P. G. Wolynes, J. Chem. Phys. **86**, 1957 (1987).
 - ¹³ M. Sparpaglione and S. Mukamel, J. Phys. Chem. **91**, 3938 (1987).
 - ¹⁴ M. Sparpaglione and S. Mukamel, J. Chem. Phys. **88**, 3263 (1988).
 - ¹⁵ M. Sparpaglione and S. Mukamel, J. Chem. Phys. **88**, 4300 (1988).
 - ¹⁶ Y. J. Yan, M. Sparpaglione, and S. Mukamel, J. Phys. Chem. **92**, 4842 (1988).
 - ¹⁷ Y. J. Yan and S. Mukamel, J. Phys. Chem. **93**, 6991 (1989).
 - ¹⁸ D. Y. Yang and S. Y. Sheu, J. Chem. Phys. **107**, 9361 (1997).
 - ¹⁹ J. Tang and S. H. Lin, J. Chem. Phys. **107**, 3485 (1997).
 - ²⁰ M. Bixon and J. Jortner, Adv. Chem. Phys. **106**, 35 (1999).
 - ²¹ W. H. Miller, Faraday Discuss. Chem. Soc. **110**, 1 (1998).
 - ²² D. Frenkel and B. Smit, *Understanding Molecular Simulation: From Algorithms to Applications*, Academic Press, London, 2nd edition, 2002.
 - ²³ E. Pollak and P. Talkner, Chaos **15**, 026116 (2005).
 - ²⁴ P. Han, R. Xu, B. Li, J. Xu, P. Cui, Y. Mo, and Y. Yan, J. Phys. Chem. B **110** (2006).

FIG. 1: Schematics of solvent environmental potentials V_a and V_b for the ET system in the donor and acceptor states, respectively, as the functions of the solvation coordinate $U \equiv V_b - V_a - E^\circ$, with E° being the ET endothermicity and $\lambda = \langle U \rangle$ the solvation energy. The classical barrierless system is that of $E^\circ + \lambda = 0$.

FIG. 2: ET rates (k) as functions of scaled solvent longitudinal relaxation time ($\tau_L/\tau_{\text{ther}}$) for the symmetric ($E^\circ = 0$) and the classical barrierless ($E^\circ + \lambda = 0$) systems at $T=298$ K, with $\lambda = 3$ kJ/mol and $V = 1$ kJ/mol. The thermal time $\tau_{\text{ther}} \equiv \hbar/(k_B T) = 10^{-1.6}$ ps at the room temperature.

FIG. 3: ET rates (k) as functions of reaction endothermicity (E°). Three values of the relative relaxation time, $\tau_L/\tau_{\text{ther}} = 0.1, 1, 10$ are used to represent low, intermediate, and high viscosity regimes.

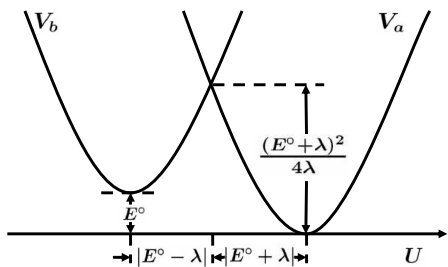


Figure 1

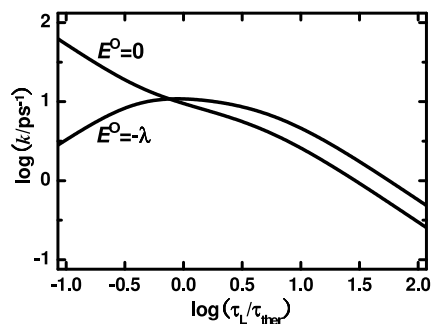


Figure 2

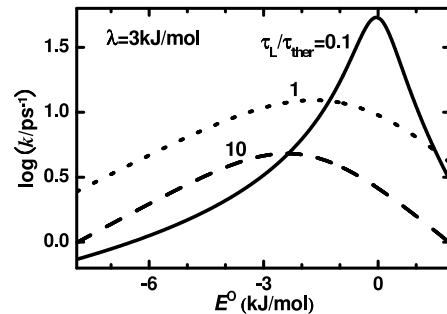


Figure 3